Towards an Information Theoretic Framework of Context-Based Offline Meta-Reinforcement Learning

 $\begin{array}{c} \textbf{Lanqing Li}^{1,2*}, \textbf{Hai Zhang}^{3*}, \textbf{Xinyu Zhang}^{4}, \textbf{Shatong Zhu}^{3}, \\ \textbf{Junqiao Zhao}^{3\dagger}, \textbf{Pheng-Ann Heng}^{1} \end{array}$

¹The Chinese University of Hong Kong ²Zhejiang Lab ³Tongji University ⁴State University of New York at Stony Brook

lanqingli1993@gmail.com, {zhanghai12138,zhushatong,zhaojunqiao}@tongji.edu.cn zhang146@cs.stonybrook.edu, pheng@cse.cuhk.edu.hk

Abstract

As a marriage between offline RL and meta-RL, the advent of offline metareinforcement learning (OMRL) has shown great promise in enabling RL agents to multi-task and quickly adapt while acquiring knowledge safely. Among which, Context-based OMRL (COMRL) as a popular paradigm, aims to learn a universal policy conditioned on effective task representations. In this work, by examining several key milestones in the field of COMRL, we propose to integrate these seemingly independent methodologies into a unified information theoretic framework. Most importantly, we show that the pre-existing COMRL algorithms are essentially optimizing the same mutual information objective between the task variable M and its latent representation Z by implementing various approximate bounds. Based on the theoretical insight and the information bottleneck principle, we arrive at a novel algorithm dubbed UNICORN, which exhibits remarkable generalization across a broad spectrum of RL benchmarks, context shift scenarios, data qualities and deep learning architectures, attaining the new state-of-the-art. We believe that our framework could open up avenues for new optimality bounds and COMRL algorithms.

1 Introduction

The ability to swiftly learn and generalize to new tasks is a hallmark of human intelligence. In pursuit of this high level of artificial intelligence (AI), the paradigm of meta-reinforcement learning (RL) proposes to train AI agents in a trial-and-error manner by interacting with multiple external environments. In order to quickly adapt to the unknown, the agents need to integrate prior knowledge with minimal experience (namely the context) collected from the new tasks or environments, without over-fitting to the new data. This meta-RL mechanism has been adopted in many applications such as games [Zhao et al., 2022a, Beck et al., 2023], robotics [Yu et al., 2020a, Kumar et al., 2021] and drug discovery [Feng et al., 2022].

However, for data collection, classical meta-RL usually requires enormous online explorations of the environments [Finn et al., 2017, Rakelly et al., 2019], which is impractical in many safety-critical scenarios such as healthcare [Gottesman et al., 2019] and autonomous driving [Shalev-Shwartz et al., 2016]. As a remedy, offline RL [Levine et al., 2020] enables agents to learn from logged experience only, therefore circumventing risky or costly online interactions. Recently, offline meta-RL (OMRL) [Li et al., 2021b, Mitchell et al., 2021, Dorfman et al., 2021] has emerged as a novel

^{*}Equal Contribution. Work done during Hai Zhang's internship at Zhejiang Lab.

[†]Corresponding author

paradigm to significantly extend the applicable range of RL by "killing two birds in one stone": it builds powerful agents that can quickly learn and adapt by meta-learning, while leveraging offline RL mechanism to ensure a safe and efficient optimization procedure. In the context of supervised or self-supervised learning, which is de facto offline, OMRL is reminiscent of the multi-task learning [Raffel et al., 2020], meta-training [Finn et al., 2017] and fine-tuning [Hu et al., 2021, Li and Liang, 2021, Lester et al., 2021] of pre-trained large models. We envision it to be a cornerstone of RL foundation models [Bommasani et al., 2021, Reed et al., 2022] in the future.

Along the line of OMRL research, context-based offline meta-reinforcement learning (COMRL) is a popular paradigm that seeks optimal meta-policy conditioning on the context of Markov Decision Processes (MDPs). Intuitively, the crux of COMRL is learning effective task representations, and therefore enabling the agent to react optimally and adaptively in various contexts. To achieve this goal, one of the earliest COMRL algorithms FOCAL [Li et al., 2021b] proposes to capture the structure of task representations by distance metric learning. From a geometric perspective, it essentially performs clustering by pushing away latent embeddings of different tasks while pulling together those from the same task, hence ensuring consistent and distinguishable task representations.

Despite its effectiveness, FOCAL is reported to be vulnerable to context shifts [Li et al., 2021a], i.e., when testing on out-of-distribution (OOD) data. Such problems are particularly challenging for OMRL, since any context shift incurred at test time can not be rectified in the fully offline setting, which may result in severely degraded generalization performance [Li et al., 2021a, Gao et al., 2023]. To alleviate the problem, follow-up works such as CORRO [Yuan and Lu, 2022] reformulates the task representation learning of COMRL as maximizing the mutual information I(Z; M) between the task variable M and its latent Z. It then approximates I(Z; M) by an InfoNCE [Oord et al., 2018] contrastive loss, where the positive and negative pairs are conditioned on identical state-action tuples (s, a). Inspired by CORRO, a recently proposed method CSRO [Gao et al., 2023] introduces an additional mutual information term between Z and (s, a). By explicitly minimizing it along with the FOCAL objective, CSRO is demonstrated to achieve the state-of-the-art (SOTA) generalization performance on various MuJoCo [Todorov et al., 2012] benchmarks.

In this paper, following the recent development and storyline of COMRL, we present a novel and unified view of several signature methods including FOCAL, CORRO and CSRO under a information theoretic framework. We first show that these algorithms are essentially optimizing different approximate bounds of the same mutual information objective I(Z,M). Then based on our proposed Unified Information Theoretic Framework of Context-Based Offline Meta-Reinforcement Learning (UNICORN), we arrive at a new COMRL optimization scheme by deriving a *unified* and *generalized* task representation learning objective in light of the information bottleneck principle [Tishby et al., 1999, Tishby and Zaslavsky, 2015]. We demonstrate experimentally that the proposed method achieves state-of-the-art in-distribution and OOD generalization performance on a wide range of RL domains, OOD settings, data qualities and model architectures. Our framework potentially provides a principled roadmap to new COMRL algorithms by seeking better optimality bounds/approximations of the objective, as well as new implementations to further combat context shift.

2 Related Works

Offline Meta-Reinforcement Learning. OMRL solves the problems of generalization and expensive data collection by meta-learning on pre-collected offline datasets. To overcome the overestimation of out-of-distribution actions [Kumar et al., 2019, Levine et al., 2020, Gao et al., 2022], offline RL usually leverages regularizations such as KL-divergence [Jaques et al., 2019], maximum mean discrepancy (MMD) [Kumar et al., 2019] and Wasserstein Distance [Gulrajani et al., 2017] to constrain the distribution mismatch between the behavior and learner policies. Moreover, a general mechanism called behavior regularized actor critic (BRAC) [Wu et al., 2019] involving value penalty and behavior regularization has proven successful in several previous studies [Li et al., 2021b, Gao et al., 2023], and is adopted in our method.

From a meta-learning perspective, the realization of OMRL can be categorized as gradient-based and context-based paradigms. Gradient-based meta-RL methods [Finn et al., 2017, Mitchell et al., 2021] embed an optimization procedure such as gradient descent into the meta-level iteration loops, which are model-agnostic but tend to reach lower asymptotic performance with less computational efficiency in practice. COMRL conditions the models on a contextual representation of MDP [Hallak

et al., 2015] generated by recurrent [Wang et al., 2016, Fakoor et al., 2020], recursive [Mishra et al., 2017, Xu et al., 2022], probabilistic [Rakelly et al., 2019, Zintgraf et al., 2019] or deterministic [Li et al., 2021b,a, Yuan and Lu, 2022] task inference modules. At test time, it leverages neural networks as universal value/policy function approximators [Schaul et al., 2015] to perform meta-adaptation by transfer learning of the task representations. Depending on the source of the testing data, fully offline [Li et al., 2021b,a, Yuan and Lu, 2022] and offline-to-online [Zhao et al., 2022b, Pong et al., 2022] COMRL have been investigated. Notwithstanding, both paradigms may suffer significant OOD as the data-collecting policies might drastically differ from the training sets. In this work, we restrict our attention to fully offline COMRL, and demonstrate the remarkable robustness of our proposed framework to context shift in this setting.

3 Method

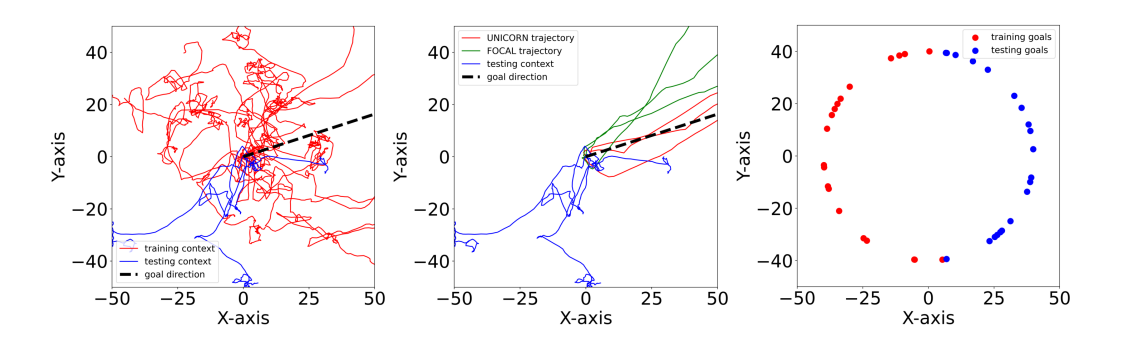


Figure 1: **Context shift of COMRL in Ant-Dir. Left**: Given a task specified by a goal direction (dashed line), the RL agent is trained on data generated by a variety of behavior policies trained on the *same* task (red). At test time, however, the context might be collected by behavior policies trained on *different* tasks (blue), causing a context shift of OOD behavior policies (Section 4.4). **Middle**: Under OOD testing context, UNICORN (red) is more robust than baselines such as FOCAL (green) in terms of navigating the Ant robot along the right direction. **Right**: Besides behavior policy, the task distribution (e.g., goal positions in Ant) can induce significant context shift (Section 5.2), which is also a challenging scenario for COMRL models to generalize.

3.1 Preliminaries and Problem Statement

We consider MDP modeled as $M=(\mathcal{S},\mathcal{A},T,R,\rho_0,\gamma)$ with state space \mathcal{S} , action space \mathcal{A} , transition function T(s'|s,a), bounded reward function R(s,a), initial state distribution $\rho_0(s)$ and discount factor $\gamma\in(0,1)$. The goal is to find a policy $\pi:\mathcal{S}\to\mathcal{A}$ to maximize the expected return. Starting from the initial state, for each time step, the agent performs an action sampled from π , then the environment updates the state with T and returns a reward with R. We denote the marginal state distribution at time t as $\mu_\pi^t(s)$. The V-function and Q-function are given by

$$V_{\pi}(s) = \sum_{t=0}^{\infty} \gamma^{t} \mathbb{E}_{s_{t} \sim \mu_{\pi}^{t}(s), a_{t} \sim \pi} [R(s_{t}, a_{t})]$$

$$(1)$$

$$Q_{\pi}(s, a) = R(s, a) + \gamma \mathbb{E}_{s' \sim T(s'|s, a)}[V_{\pi}(s')].$$
(2)

In this paper, we restrict to scenarios where tasks share the same state and action space while differing in reward and transition functions, with each OMRL task defined as an instance of MDP: $M^i = (\mathcal{S}, \mathcal{A}, T^i, R^i, \rho_0, \gamma) \in \mathcal{M}$, where \mathcal{M} is the set of all possible MDPs to be considered. For each task index i, the offline dataset $X^i = \{(s^i_j, a^i_j, r^i_j, {s'}^i_j)\}$ is collected by a behavior policy π^i_β . For meta-learning, given a trajectory segment $c^i_{1:n} = \{(s^i_j, a^i_j, r^i_j, {s'}^i_j)\}_{j=1}^n$ of length n as the context

of M^i , COMRL employs a context encoder $q_{\phi}(z|c_{1:n}^i)$ to obtain the latent representation z^i of task M^i . If z contains enough information about the task identity, COMRL can be treated as a special case of RL on partially-observed MDP [Kaelbling et al., 1998], where z is interpreted as a faithful representation of the unobserved state. By conditioning on z, the learning of universal policy $\pi_{\theta}(\cdot|s,z)$ and value function $V_{\pi}(s,z)$ [Schaul et al., 2015] become regular RL, and optimality can be attained by Bellman updates with theoretical guarantees. To this end, FOCAL [Li et al., 2021b] proposes to decouple COMRL into the upstream task representation learning and downstream offline RL. For the former, FOCAL effectively clusters task embeddings by metric learning:

$$\mathcal{L}_{\text{FOCAL}} = \min_{\phi} \mathbb{E}_{i,j} \left\{ \mathbf{1} \{ i = j \} || \mathbf{z}^i - \mathbf{z}^j ||_2^2 + \mathbf{1} \{ i \neq j \} \frac{\beta}{||\mathbf{z}^i - \mathbf{z}^j ||_2^n + \epsilon} \right\}.$$
(3)

However, it is empirically shown that FOCAL struggles to generalize in the presence of context shift [Li et al., 2021a]. This problem has been formulated in several earliest studies of OMRL. Li et al. [2020] observed that when there are large divergence between the state-action distributions of the offline datasets, due to shortcut learning [Geirhos et al., 2020], the task encoder may learn to ignore the causal information like rewards and *spuriously correlate* primarily state-action pairs to the task identity, leading to poor generalization performance. Dorfman et al. [2021] concurrently identified a related problem which they termed MDP ambiguity in the context of Bayesian offline RL. An example is illustrated in Figure 1. The problem is further exacerbated in the fully offline setting, as the testing distribution is fixed and cannot be augmented by online exploration, allowing no theoretical guarantee for the context shift.

To mitigate context shift, a subsequent algorithm CORRO [Yuan and Lu, 2022] proposes to optimize a lower bound of $I(\mathbf{Z}; \mathbf{M})$ in the form of an InfoNCE [Oord et al., 2018] contrastive loss

$$\mathcal{L}_{\text{CORRO}} = \min_{\phi} \mathbb{E}_{\boldsymbol{x}, \boldsymbol{z}} \left[-\log \left(\frac{h(\boldsymbol{x}, \boldsymbol{z})}{\sum_{M^* \in \mathcal{M}} h(\boldsymbol{x}^*, \boldsymbol{z})} \right) \right], \tag{4}$$

where $\boldsymbol{x}=(s,\boldsymbol{a},r,s'), \, \boldsymbol{z}\sim q_{\phi}(\boldsymbol{z}|\boldsymbol{x}), \, h(\boldsymbol{x},\boldsymbol{z})=\frac{P(\boldsymbol{z}|\boldsymbol{x})}{P(\boldsymbol{z})}\approx \frac{q_{\phi}(\boldsymbol{z}|\boldsymbol{x})}{P(\boldsymbol{z})}, \, \text{and} \, \boldsymbol{x}^*=(s,\boldsymbol{a},r^*,s'^*)$ as a transition tuple generated for task $M^*\in\mathcal{M}$ conditioned on the same (s,\boldsymbol{a}) . To further combat the spurious correlation between the task representation and behavior-policy-induced state-actions, a recently proposed method CSRO [Gao et al., 2023] introduces a CLUB upper bound [Cheng et al., 2020] of the mutual information between \boldsymbol{z} and (s,\boldsymbol{a}) , to regularize the FOCAL objective:

$$\mathcal{L}_{\text{CSRO}} = \min_{\phi} \left\{ \mathcal{L}_{\text{FOCAL}} + \lambda L_{\text{CLUB}} \right\} \tag{5}$$

$$L_{\text{CLUB}} = \mathbb{E}_i \left[\log q_{\phi}(\boldsymbol{z}_i | \boldsymbol{s}_i, \boldsymbol{a}_i) - \mathbb{E}_j \left[\log q_{\phi}(\boldsymbol{z}_j | \boldsymbol{s}_i, \boldsymbol{a}_i) \right] \right]. \tag{6}$$

In the next section, we will show how these algorithms are inherently connected and can be further improved under our proposed unified information theoretic framework.

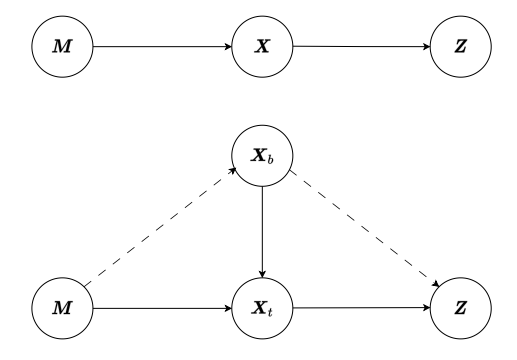
3.2 A Unified Information Theoretic Framework

We start with a formal definition of task representation learning in COMRL:

Definition 3.1. Given an input context variable $X \in \mathcal{X}$ and its associated task/MDP random variable $M \in \mathcal{M}$, task representation learning in COMRL aims to find a minimal sufficient statistics Z of X with respect M.

In pure statistical terms, Definition 3.1 implies that an ideal representation Z is the simplest mapping of X that captures the mutual information I(X; M). We therefore assume the following dependency structures in terms of directed graphical models:

Assumption 3.2. The dependency graphs of COMRL are given by



satisfying $I(\mathbf{Z}; \mathbf{M}; \mathbf{X}_b) \geq 0$, where \mathbf{X}_b and \mathbf{X}_t are the behavior-related (\mathbf{s}, \mathbf{a}) -component and task-related (\mathbf{s}', r) -component of the context \mathbf{X} , with $\mathbf{X} = (\mathbf{X}_t, \mathbf{X}_b)$.

For the first graph, $M \to X \to Z$ forms a Markov chain, which satisfies I(Z; M|X) = 0. To interpret the second graph, given an MDP $M \sim M$, the state-action component of X is fully captured by the behavior policy $\pi_{\beta} \colon s \sim \mu_{\pi_{\beta}}(s), a \sim \pi_{\beta}$. We therefore define it as the *behavior-related* component, which should be *minimally* causally related (dashed lines) to M and Z. Moreover, when X_b is given, X_t is fully characterized by the transition function $T:(s,a)\to s'$ and reward function $R:(s,a)\to r$ of M, which should be *maximally* causally related (solid lines) to M and Z and therefore be defined as the *task-related* component. Accordingly, we name $I(Z;X_t|X_b)$ and $I(Z;X_b)$ the *primary* and *lesser* causality in our problem respectively. With this prior knowledge and assumption, we present the central theorem of this paper:

Theorem 3.3. Let \equiv denote equality up to a constant,

$$\underbrace{I(oldsymbol{Z}; oldsymbol{X}_t | oldsymbol{X}_b)}_{primary\ causality} \quad \leq \quad I(oldsymbol{Z}; oldsymbol{M}) \quad \leq \quad \underbrace{I(oldsymbol{Z}; oldsymbol{X})}_{primary\ +\ lesser\ causality}$$

holds up to a constant, where

- 1. $\mathcal{L}_{FOCAL} \equiv -I(\boldsymbol{Z}; \boldsymbol{X}).$
- 2. $\mathcal{L}_{CORRO} \equiv -I(\boldsymbol{Z}; \boldsymbol{X}_t | \boldsymbol{X}_b)$.
- 3. $\mathcal{L}_{CSRO} \geq (\lambda 1)I(\mathbf{Z}; \mathbf{X}) \lambda I(\mathbf{Z}; \mathbf{X}_t | \mathbf{X}_b)$.

Proof. See Appendix B, Theorem B.1.

Theorem 3.3 induces several key observations. Firstly, the FOCAL and CORRO objective operates as an upper bound and a lower bound of the relevant information I(Z; M) respectively. Since one would like to maximize I(Z; M) according to Definition 3.1, CORRO, which maximizes a lower bound $I(Z; X_t | X_b)$, can effectively optimize I(Z; M) with theoretical guarantees. However, FOCAL which maximizes an upper bound $I(Z; X_t, X_b)$ is not guaranteed to optimize I(Z; M). Mathematically since $I(Z; X) = I(Z; X_t | X_b) + I(Z; X_b)$, maximizing the FOCAL objective may also increase the lesser causality $I(Z; X_b)$, which is not ideal since it contains spurious correlation between the task representation Z and behavior policy π_{β} . This explains why FOCAL is less robust to context shift compared to CORRO.

Secondly, CSRO as a latest COMRL algorithm, inherently optimizes a linear combination of the FOCAL and CORRO objectives. In the $0 \le \lambda \le 1$ regime, the CSRO objective becomes a convex interpolation of the upper bound $I(\boldsymbol{Z}; \boldsymbol{X})$ and the lower bound $I(\boldsymbol{Z}; \boldsymbol{X}_t | \boldsymbol{X}_b)$ of $I(\boldsymbol{Z}; \boldsymbol{M})$, which may form a tighter bound on the real objective $I(\boldsymbol{Z}; \boldsymbol{M})$. This explains the improved performance of CSRO compared to FOCAL and CORRO.

3.3 UNICORN: Implementation of The Information Bottleneck Principle on COMRL

Given Definition 3.1 of the task representation learning, we now further generalize the pre-existing COMRL algorithms based on the information bottleneck principle [Tishby et al., 2000, Tishby

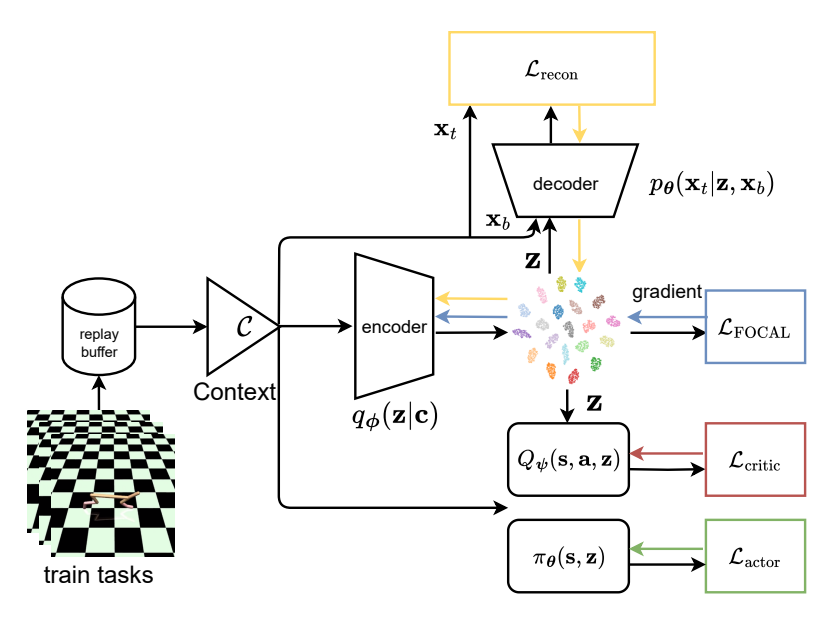


Figure 2: Meta-training procedure of UNICORN. Built upon the classic COMRL methods FOCAL, UNICORN implements the information bottleneck principle by jointly optimizing the FOCAL loss and a reconstruction loss, using a variational auto-encoder to obtain robust task representation z.

and Zaslavsky, 2015]. Namely, finding an optimal task representation Z can be formulated as the minimization of the following Lagrangian

$$\mathcal{L}_{IB} = I(\mathbf{Z}; \mathbf{X}) - \beta I(\mathbf{Z}; \mathbf{M}) \tag{7}$$

subject to the Markov chain constraint. The positive Lagrange multiplier β acts as a tradeoff parameter between the complexity/rate of the representation, $R = I(\mathbf{Z}; \mathbf{X})$, and the amount of preserved relevant information, $I_M = I(\mathbf{Z}; \mathbf{M})$. For implementation, the first term is just FOCAL loss by Theorem 3.3, whereas we propose to approximate the second term as a convex combination of the FOCAL and CORRO loss, analogous to CSRO:

$$I(Z; M) \approx \alpha I(Z; X) + (1 - \alpha)I(Z; X_t | X_b),$$
 (8)

where $0 \le \alpha \le 1$. Substituting Eqn 8 into 7, we may rescale \mathcal{L}_{IB} as

$$\mathcal{L}_{IB} = -\left(I(\boldsymbol{Z}; \boldsymbol{X}_t | \boldsymbol{X}_b) + \frac{\alpha\beta - 1}{(1 - \alpha)\beta}I(\boldsymbol{Z}; \boldsymbol{X})\right). \tag{9}$$

For implementation of $I(\mathbf{Z}; \mathbf{X}_t | \mathbf{X}_b)$, however, it would require additional approximations such as generating negative samples for contrastive learning using a trained model in CORRO, or using a CLUB upper bound of the mutual information in CSRO. Instead, we propose to rewrite it according to the chain rule of mutual information [Yeung, 2008]:

$$I(\mathbf{Z}; \mathbf{X}_t | \mathbf{X}_b) = I(\mathbf{X}_t; \mathbf{Z}, \mathbf{X}_b) - I(\mathbf{X}_t; \mathbf{X}_b)$$

$$\equiv I(\mathbf{X}_t; \mathbf{Z}, \mathbf{X}_b),$$
(10)

since $I(X_t; X_b)$ is a constant when X_t and X_b are drawn from a fixed distribution as in offline RL. Moreover, by definition of mutual information:

$$I(\boldsymbol{X_t}; \boldsymbol{Z}, \boldsymbol{X_b}) = \int p(\boldsymbol{x_t}, \boldsymbol{x_b}) p(\boldsymbol{z}|\boldsymbol{x_t}, \boldsymbol{x_b}) \log \frac{p(\boldsymbol{x_t}|\boldsymbol{z}, \boldsymbol{x_b})}{p(\boldsymbol{x_t})}$$

$$\equiv \int p(\boldsymbol{x_t}, \boldsymbol{x_b}) p(\boldsymbol{z}|\boldsymbol{x_t}, \boldsymbol{x_b}) \log p(\boldsymbol{x_t}|\boldsymbol{z}, \boldsymbol{x_b})$$

$$\simeq \int_{\boldsymbol{x_t}, \boldsymbol{x_b}, \boldsymbol{z}} \underbrace{q_{\boldsymbol{\phi}}(\boldsymbol{z}|\boldsymbol{x_t}, \boldsymbol{x_b}) \log p_{\boldsymbol{\theta}}(\boldsymbol{x_t}|\boldsymbol{z}, \boldsymbol{x_b})}_{\text{decoder}}$$

$$= \mathbb{E}_{q_{\boldsymbol{\phi}}(\boldsymbol{z}|\boldsymbol{x_t}, \boldsymbol{x_b})} \left[\log p_{\boldsymbol{\theta}}(\boldsymbol{x_t}|\boldsymbol{z}, \boldsymbol{x_b}) \right], \tag{11}$$

which induces an *unbiased* estimator of $I(X_t; Z, X_b)$ by reconstructing X_t with a decoder network $p_{\theta}(\cdot|z, x_b)$ conditioning on Z and X_b , reminiscent of VAE [Kingma and Welling, 2014]. We therefore implement the objective of our proposed algorithm UNICORN as a linear combination of this reconstruction loss $\mathcal{L}_{\text{recon}} := -I(X_t; Z, X_b)$ and the FOCAL loss $\mathcal{L}_{\text{FOCAL}} = -I(Z; X)$:

$$\mathcal{L}_{\text{UNICORN}} := \mathcal{L}_{IB} = \mathcal{L}_{\text{recon}} + \frac{\alpha\beta - 1}{(1 - \alpha)\beta} \mathcal{L}_{\text{FOCAL}}$$

$$= -\left(I(\boldsymbol{X}_t; \boldsymbol{Z}, \boldsymbol{X}_b) + \frac{\alpha\beta - 1}{(1 - \alpha)\beta} I(\boldsymbol{Z}; \boldsymbol{X})\right). \tag{12}$$

UNICORN can be interpreted as a generalization of the FOCAL and CORRO objectives by effectively striking a balance between the primary causality $I(\mathbf{Z}; \mathbf{X}_t | \mathbf{X}_b)$ and the lesser causality $I(\mathbf{Z}; \mathbf{X}_b)$. Figure 2 gives an overview of our framework, which enjoys three core advantages:

- Robustness and bias-reduction. By optimizing a reconstruction loss $I(X_t; Z, X_b)$ equivalent to the CORRO objective $I(Z; X_t | X_b)$, UNICORN mitigates the spurious correlation in FOCAL, leading to more robust task representation Z. It is also verified in Section 4.5 that UNICORN is robust to a wide range of data qualities. Moreover, the unbiased estimator in Eqn 11 circumvents additional approximations as in CORRO and CSRO, making UNICORN a bias-reduced and improved version of previous SOTAs.
- Broader applicability domain. Unlike FOCAL/CORRO which assumes uniform task distribution, the unbiased estimator in Eqn 11 can be efficiently implemented by Monte Carlo sampling on offline datasets drawn from any distribution. Additionally, we will show in Section 5.1 that UNICORN is transferable to other model architectures such as Decision Transformer (DT).
- General and unified paradigm. Derived from the general information bottleneck principle, our framework encompasses a series of milestones in COMRL including FOCAL, CORRO, CSRO and a concurrent method GENTLE [Zhou et al., 2023], which solely optimizes the reconstruction loss with a similar implementation. A unified picture of these pre-existing methods being special cases of UNICORN in the α - β plane is depicted in Figure 3. A hyper-parameter study showing the effect of the UNICORN feasible region is presented in Appendix C.1. Moreover, the decoder $p_{\theta}(x_t|z,x_b)$ can operate as a model of the MDP to generate additional data using customized latent z, which is explored in Section 5.2. In summary, UNICORN not only provides a unified framework of model-free COMRL, it may also be exploited and lead to novel model-based algorithms.

4 Experiments

Our main experiments are organized to address three primary inquiries regarding the core advantages of UNICORN: (1) How does UNICORN perform on in-distribution tasks (**bias-reduction**)? (2) How well can UNICORN generalize to data collected by OOD behavior policies (**robustness**)? (3) Can UNICORN outperform consistently across datasets of different qualities (**robustness**)? The performance are measured by the average return across all test tasks.

4.1 Environments and Datasets

We adopt MuJoCo [Todorov et al., 2012] and MetaWorld [Yu et al., 2020a] benchmarks to evaluate our method.

HalfCheetah-Dir, HalfCheetah-Vel, Ant-Dir are multi-task MuJoCo benchmarks where tasks differ in *reward function*. For HalfCheetah-Dir and Ant-Dir, the agent is rewarded with high velocity along the goal direction. For HalfCheetah-Vel, the agent receives an L_2 penalty with respect to the target velocity.

Hopper-Param, Walker-Param are multi-task MuJoCo benchmarks where tasks differ in *transition dynamics*. The physical parameters of body mass, inertia, damping, and friction vary for each task.

Reach is a multi-task MetaWorld benchmark where tasks differ in *reward function*. The agent controls the end-effector to reach a target position in 3D space.

Following the protocol of CORRO, we sample 20 training tasks and 20 testing tasks from the

task distribution. We train SAC agent [Haarnoja et al., 2018] independently for each task and collect offline datasets of mixed quality using all logged behavior policies.

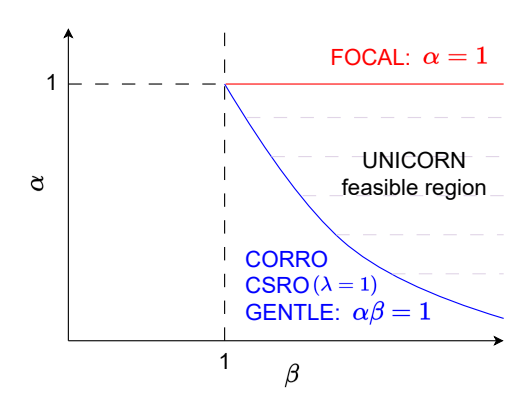


Figure 3: The hyper-parameter plane of UNI-CORN. Empirically, we find that UNICORN works properly only when $(\alpha\beta-1)/(1-\alpha)\beta>0$, which further constrains the feasible region of UNI-CORN (shaded) to be bounded by $\alpha\beta\geq 1$, $\alpha\leq 1$ and $\beta\geq 1$. Intriguingly, pre-existing methods FO-CAL (red) and CORRO/CSRO/GENTLE (blue) constitute the two boundaries of the feasible region, which can therefore be interpreted as special cases of UNICORN.

4.2 Baselines

We compare UNICORN with six competitive OMRL algorithms. These baselines are categorized as context-based, gradient-based or transformer-based methods.

FOCAL, CORRO, CSRO are context-based methods which can be seen as special cases or approximations of UNICORN, see details in Section 3.

Supervised is a *context-based* method, directly using actor-critic loss to train the policy/value networks and task encoder end-to-end. We find it a competitive baseline across all benchmarks.

MACAW [Mitchell et al., 2021] is a *gradient-based* method, using supervised advantage-weighted regression for both the inner and outer loop of meta-training.

Prompt-DT [Xu et al., 2022] is a *transformer-based* method, taking context as the prompt of a Decision Transformer (DT) [Chen et al., 2021, Janner et al., 2021] to solve OMRL as a conditional sequence modeling problem.

We perform our evaluation in a few-shot manner. For gradient-based methods, we first update the meta-policy with a batch of context, then evaluate the agent. For transformer-based methods, we utilize z inferred from a batch of context as the prompt to condition the auto-regressive rollout.

4.3 Few-Shot Generalization to In-Distribution Data

Table 1: Average testing returns of UNICORN against baselines on datasets collected by IID and OOD behavior policies. Each result is averaged by 6 random seeds. The best is **bolded** and the second best is underlined.

Algorithm	HalfCheetah-Dir		HalfCheetah-Vel		Ant-Dir		Hopper-Param		Walker-Param		Reach	
	IID	OOD	IID	OOD	IID	OOD	IID	OOD	IID	OOD	IID	OOD
UNICORN	1312.59±31.72	1301.17±25.98	-21.88±0.65	-93.57±4.85	266.85±14.54	235.55±17.69	315.90±5.67	304.45±10.88	407.83±75.58	392.48±74.45	2774.67±241.04	2603.68±182.85
CSRO	1180.48±228.10	458.08±253.00	-27.98±0.90	-102.44±5.17	276.18±19.37	233.33±12.37	309.63±6.50	301.12±9.99	310.47±58.29	278.94±65.37	2719.50±234.55	2800.93±182.06
CORRO	704.20±449.46	244.95±145.83	-37.11±2.60	-112.29±1.62	147.93±12.85	120.52±12.48	283.04±7.89	271.48±12.79	277.07±37.91	213.43±48.33	2467.83±174.57	2321.87±327.19
FOCAL	1186.03±271.58	860.58±252.96	-22.22±0.88	-96.72±1.69	217.10±29.14	173.16±24.37	301.84±4.48	296.87±12.76	308.05±98.42	286.34±91.08	2423.67±255.95	2315.56±303.03
Supervised	961.62±355.84	781.51±429.12	-23.81±0.71	-104.31±0.65	237.52±38.81	202.19±37.56	306.54±9.99	293.65±7.99	256.52±60.39	209.64±27.72	2489.37±248.05	2283.26±205.36
MACAW	1154.83±10.11	449.56±6.54	-56.04±2.42	-188.44±0.91	26.29±2.80	0.18±0.31	218.52±6.01	205.39±2.47	141.25±8.83	129.63±5.09	2430.67±157.42	1728.01±78.98
Prompt-DT	1176.54±39.64	-25.10±8.74	-118.14±65.59	-248.64±21.38	1.00±0.38	0.04±0.11	234.19±5.35	202.51±4.96	184.73±8.57	155.78±16.64	2164.86±85.20	1895.51±110.64

Figure 4 illustrates the learning curves of UNICORN vs. all baselines. IID entries of Table 1 depicts the performance of in-distribution generalization where the context for each task is collected by

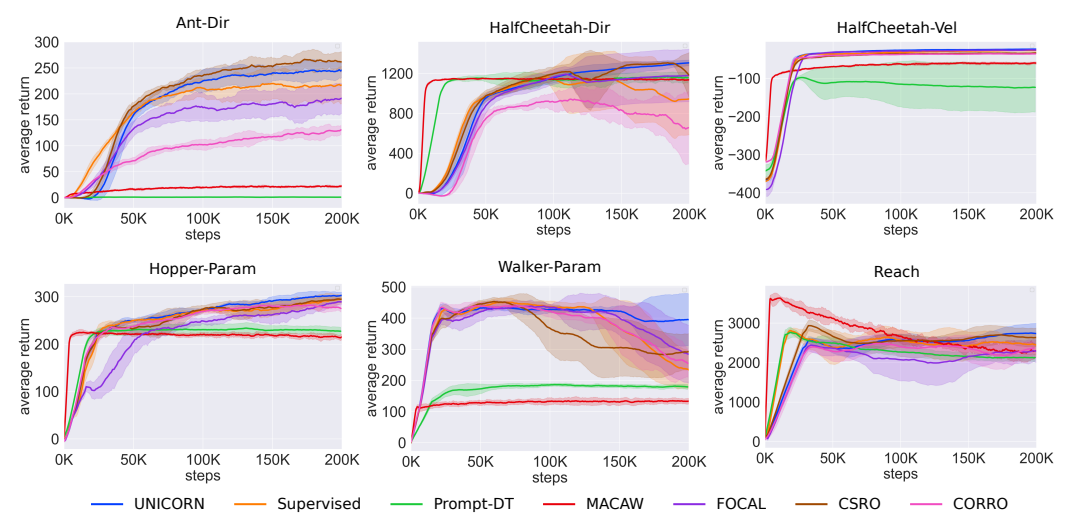


Figure 4: **Testing returns of UNICORN against baselines on six benchmarks.** Solid curves refer to the mean performance of trials over 6 random seeds, and the shaded areas characterize the standard deviation of these trials.

the behavior policies trained on the *same* task. The results demonstrate that UNICORN almost unanimously achieves SOTA performance across all benchmarks. The observation that FOCAL, CORRO, and CSRO achieve asymptotic performance close to UNICORN is also expected, since they are special cases of UNICORN according to our theory. Notably, UNICORN exhibits remarkable stability, especially on HalfCheetah-Dir and Walker-Param, where the other context-based methods suffer a significant performance decline during the later training process. Although the gradient-based MACAW and the transformer-based Prompt-DT show faster convergence, their asymptotic performance leaves much to be desired. Moreover, the average training time for MACAW is almost three times longer than the context-based methods.

4.4 Few-Shot Generalization to Out-of-Distribution Behavior Policies

Denote by $\{\pi_{\beta}^{i,t}\}_{i,t}$ the checkpoints of behavior policies for all tasks logged during data collection (i.e., training SAC agents), where i refers to the task index and t represents training iteration. For each test task M^j , we use *every* individual behavior policy in $\{\pi_{\beta}^{i,t}\}_{i,t}$ to collect the OOD contexts and the conditioned rollouts, as visualized in Figure 1. The OOD testing performance is measured by averaging returns across all testing tasks, as shown in the OOD entries of Table 1. While all methods suffer notable decline when facing OOD context, UNICORN maintains the strongest performance by a large margin. Another observation is that the context-based methods are in general significantly more robust compared to the gradient-based MACAW and transformer-based Prompt-DT, which suggests that context-based paradigm should be prioritized for research of generalizable OMRL. This also delineates the storyline of COMRL development from 2021 to date

$$\begin{array}{c} \text{FOCAL} \rightarrow \text{CORRO} \rightarrow \text{CSRO} \rightarrow \text{UNICORN} \\ \text{\tiny (2021)} & \text{\tiny (2022)} \end{array}$$

as a roadmap for pursuing more robust and generalizable task representation learning for COMRL.

4.5 Influence of Data Quality

To test whether the UNICORN framework can be applied to different data distributions, we collect three types of datasets whose size is equal to the mixed dataset used in Section 4.3 and 4.4: random, medium and expert, which are characterized by the quality of the behavior policies. Each dataset is collected by one SAC agent. For random datasets, the SAC agent is randomly initialized and untrained.

Table 2: **UNICORN vs. baselines on Ant-Dir datasets of various qualities.** Each result is averaged by 6 random seeds. The best is **bolded** and the second best is <u>underlined</u>.

Algorithm	Ran	dom	Med	lium	Expert		
Algorium	IID	OOD	IID	OOD	IID	OOD	
UNICORN	81.31±17.80	62.20±6.15	219.86±23.04	242.74±10.40	278.82±10.46	261.83±13.49	
CSRO	1.55±2.65	-0.20 ± 0.52	165.65±9.89	198.15±17.35	251.77±39.16	201.57±45.29	
CORRO	0.87 ± 0.53	-0.05 ± 0.06	8.16±5.02	-7.01±2.37	-3.90±9.59	-13.59±9.06	
FOCAL	67.00±26.33	43.65±10.08	171.10±84.26	187.06±86.45	229.02±42.07	246.27±20.21	
Supervised	64.97±5.57	46.90±11.86	149.21±50.21	109.85±80.09	249.11±33.47	214.55±59.56	
MACAW	3.412±0.74	-0.27±0.25	27.69±2.17	1.34±0.75	87.86±42.69	0.64±1.49	
Prompt-DT	0.54±0.29	0.02±0.09	2.14±4.36	0.33±0.57	77.94±14.67	1.24±2.18	

As shown in Table 2, UNICORN demonstrates SOTA performance on all types of datasets. Notably, despite CSRO having better IID results than UNICORN on Ant-Dir under the mixed data distribution, UNICORN surpasses CSRO by a large margin under the narrow data distribution (medium and expert) and random data distribution.

We observe that CORRO fails on all three datasets. This may be due to the reliance of CORRO on the negative sample generator. Under narrow data distribution or poor random data distribution, it might be more challenging to generate negative samples of good quality. As for Prompt-DT, its performance improves significantly with increased data quality, which is expected since the decision transformer adopts a behavior-cloning-like supervised learning style.

5 Discussion

This section presents more empirical evidence on the broader applicability of the UNICORN framework.

5.1 Is UNICORN Model-Agnostic?

Since UNICORN tackles task representation learning from a general information theoretic perspective, it is in principle *model-agnostic*. Hence a straightforward idea is to transfer UNICORN to other model architectures like DT, which we envision to be a promising backbone for large-scale training of RL foundation models.

We employ a simple implementation by embedding the task representation vector z as the first token in sequence to prompt the learning and generation of DT. Instead of the unlearnable prompt used in the original Prompt-DT, we enforce task representation learning of the prompt by optimizing $\mathcal{L}_{\text{UNICORN}}$ and $\mathcal{L}_{\text{FOCAL}}$. We name these DT implementations as UNICORN-DT and FOCAL-DT respectively.

As shown in Table 3 and Figure 8, applying UNICORN and FOCAL on DT results in significant improvement in both IID and OOD generalization, with UNICORN being the superior option. Despite the gap between our implementation of UNICORN-DT and its MLP counterpart in terms of asymptotic performance, we expect UNICORN-DT to extrapolate favorably in the regime of greater dataset size and model parameters due to the scaling law of transformer [Kaplan et al., 2020] and DT [Lee et al., 2022]. We leave this verification to future work.

Table 3: **DT implementation of COMRL on HalfCheetah-Dir and Hopper-Param.** Each result is averaged by 6 random seeds.

Algorithm	HalfChe	etah-Dir	Hopper-Param		
Algorium	IID	OOD	IID	OOD	
UNICORN	1312.59±31.72	1301.17±25.98	315.90±5.67	304.45±10.88	
UNICORN-DT FOCAL-DT Prompt-DT	1233.19±10.42 1208.58±33.38 1176.54±39.64	1185.76±42.71 652.14±35.86 -25.10±8.74	303.66±3.51 293.25±4.17 234.19±5.35	290.88±3.68 283.86±4.81 202.51±4.96	

5.2 Can UNICORN be Exploited for Model-Based Paradigms?

As alluded in Section 3.3, UNICORN can potentially enable a model-based paradigm by generating data using the decoder $p_{\theta}(\boldsymbol{x}_t|\boldsymbol{z},\boldsymbol{x}_b)$ and customized latent \boldsymbol{z} , which can be especially useful for generalization to OOD tasks. We implement this idea on Ant-Dir by sorting the tasks according to the polar angle of their goal direction ($\theta \in [0,2\pi)$), and construct task-level OOD by taking 20 consecutive tasks in the middle for training and the rest for testing (Figure 1). Gaussian noise $\boldsymbol{\epsilon}$ is applied to the real task representation \boldsymbol{z} and $(\boldsymbol{s},\boldsymbol{a},\boldsymbol{z}+\boldsymbol{\epsilon})$ is then fed to the decoder to generate (\boldsymbol{s}',r) . The imaginary rollouts $\{(\boldsymbol{s}_t,\boldsymbol{a}_t,\boldsymbol{s}_t',r_t)\}_{t=1}^n$ are used during the training of RL agent. We adopt the conventional ensemble technique in model-based RL [Yu et al., 2020b, Zhang et al., 2023] to stabilize the training process.

As shown in Figure 5, UNICORN-enabled model-based RL is the only method to achieve positive performance in this extremely challenging scenario where context shift is induced by OOD tasks.

6 Conclusion

In this paper, we unify three major context-based offline meta-RL algorithms, FOCAL, CORRO and CSRO (potentially a lot more) into a single framework based on the information bottleneck principle. Our theory offers valuable insight on how these methods are inherently connected and incrementally evolved in pursuit of better generalization against context shift. Based on the proposed framework, we arrive at a novel algorithm called UNICORN which is demonstrated to be remarkably robust and broadly applicable through extensive experiments. We believe our study offers potential for new implementations, optimality bounds and algorithms for both fully offline and offline-to-online COMRL paradigms. We leave these directions for future work.

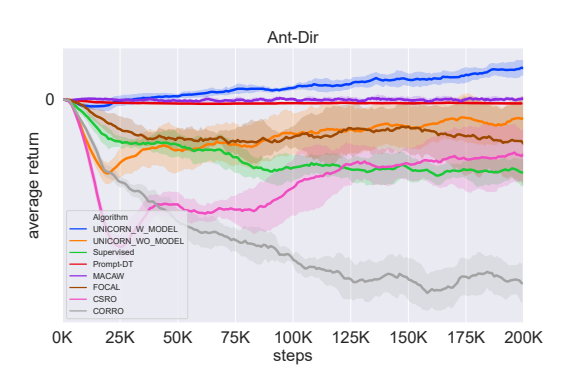


Figure 5: **Testing returns for OOD tasks.** The learning curve is averaged by 6 random seeds.

References

- J. Beck, R. Vuorio, E. Z. Liu, Z. Xiong, L. Zintgraf, C. Finn, and S. Whiteson. A survey of meta-reinforcement learning. *arXiv preprint arXiv:2301.08028*, 2023.
- R. Bommasani, D. A. Hudson, E. Adeli, R. Altman, S. Arora, S. von Arx, M. S. Bernstein, J. Bohg, A. Bosselut, E. Brunskill, et al. On the opportunities and risks of foundation models. *arXiv preprint arXiv:2108.07258*, 2021.
- L. Chen, K. Lu, A. Rajeswaran, K. Lee, A. Grover, M. Laskin, P. Abbeel, A. Srinivas, and I. Mordatch. Decision transformer: Reinforcement learning via sequence modeling. *Advances in neural information processing systems*, 34:15084–15097, 2021.
- P. Cheng, W. Hao, S. Dai, J. Liu, Z. Gan, and L. Carin. Club: A contrastive log-ratio upper bound of mutual information. In *International conference on machine learning*, pages 1779–1788. PMLR, 2020.
- R. Dorfman, I. Shenfeld, and A. Tamar. Offline meta reinforcement learning-identifiability challenges and effective data collection strategies. *Advances in Neural Information Processing Systems*, 34: 4607–4618, 2021.
- R. Fakoor, P. Chaudhari, S. Soatto, and A. J. Smola. Meta-q-learning. In *International Conference on Learning Representations*, 2020.
- L. Feng, P. Nouri, A. Muni, Y. Bengio, and P.-L. Bacon. Designing biological sequences via meta-reinforcement learning and bayesian optimization. *arXiv* preprint arXiv:2209.06259, 2022.

- C. Finn, P. Abbeel, and S. Levine. Model-agnostic meta-learning for fast adaptation of deep networks. In *International conference on machine learning*, pages 1126–1135. PMLR, 2017.
- C. Gao, K. Xu, K. Zhou, L. Li, X. Wang, B. Yuan, and P. Zhao. Value penalized q-learning for recommender systems. In *Proceedings of the 45th International ACM SIGIR Conference on Research and Development in Information Retrieval*, pages 2008–2012, 2022.
- Y. Gao, R. Zhang, J. Guo, F. Wu, Q. Yi, S. Peng, S. Lan, R. Chen, Z. Du, X. Hu, et al. Context shift reduction for offline meta-reinforcement learning. In *Thirty-seventh Conference on Neural Information Processing Systems*, 2023.
- R. Geirhos, J.-H. Jacobsen, C. Michaelis, R. Zemel, W. Brendel, M. Bethge, and F. A. Wichmann. Shortcut learning in deep neural networks. *Nature Machine Intelligence*, 2(11):665–673, 2020.
- O. Gottesman, F. Johansson, M. Komorowski, A. Faisal, D. Sontag, F. Doshi-Velez, and L. A. Celi. Guidelines for reinforcement learning in healthcare. *Nature medicine*, 25(1):16–18, 2019.
- I. Gulrajani, F. Ahmed, M. Arjovsky, V. Dumoulin, and A. C. Courville. Improved training of wasserstein gans. Advances in neural information processing systems, 30, 2017.
- T. Haarnoja, A. Zhou, P. Abbeel, and S. Levine. Soft actor-critic: Off-policy maximum entropy deep reinforcement learning with a stochastic actor. In *International conference on machine learning*, pages 1861–1870. PMLR, 2018.
- A. Hallak, D. Di Castro, and S. Mannor. Contextual markov decision processes. *arXiv preprint arXiv:1502.02259*, 2015.
- E. J. Hu, P. Wallis, Z. Allen-Zhu, Y. Li, S. Wang, L. Wang, W. Chen, et al. Lora: Low-rank adaptation of large language models. In *International Conference on Learning Representations*, 2021.
- M. Janner, Q. Li, and S. Levine. Offline reinforcement learning as one big sequence modeling problem. *Advances in neural information processing systems*, 34:1273–1286, 2021.
- N. Jaques, A. Ghandeharioun, J. H. Shen, C. Ferguson, A. Lapedriza, N. Jones, S. Gu, and R. Picard. Way off-policy batch deep reinforcement learning of implicit human preferences in dialog. *arXiv* preprint arXiv:1907.00456, 2019.
- L. P. Kaelbling, M. L. Littman, and A. R. Cassandra. Planning and acting in partially observable stochastic domains. *Artificial intelligence*, 101(1-2):99–134, 1998.
- J. Kaplan, S. McCandlish, T. Henighan, T. B. Brown, B. Chess, R. Child, S. Gray, A. Radford, J. Wu, and D. Amodei. Scaling laws for neural language models. *arXiv preprint arXiv:2001.08361*, 2020.
- D. P. Kingma and M. Welling. Auto-encoding variational bayes. In Y. Bengio and Y. LeCun, editors, 2nd International Conference on Learning Representations, ICLR 2014, Banff, AB, Canada, April 14-16, 2014, Conference Track Proceedings, 2014. URL http://arxiv.org/abs/1312.6114.
- A. Kumar, J. Fu, M. Soh, G. Tucker, and S. Levine. Stabilizing off-policy q-learning via bootstrapping error reduction. *Advances in Neural Information Processing Systems*, 32, 2019.
- A. Kumar, Z. Fu, D. Pathak, and J. Malik. Rma: Rapid motor adaptation for legged robots. *arXiv* preprint arXiv:2107.04034, 2021.
- K.-H. Lee, O. Nachum, M. S. Yang, L. Lee, D. Freeman, S. Guadarrama, I. Fischer, W. Xu, E. Jang, H. Michalewski, et al. Multi-game decision transformers. *Advances in Neural Information Processing Systems*, 35:27921–27936, 2022.
- B. Lester, R. Al-Rfou, and N. Constant. The power of scale for parameter-efficient prompt tuning. In *Proceedings of the 2021 Conference on Empirical Methods in Natural Language Processing*, pages 3045–3059, 2021.
- S. Levine, A. Kumar, G. Tucker, and J. Fu. Offline reinforcement learning: Tutorial, review, and perspectives on open problems. *arXiv* preprint arXiv:2005.01643, 2020.

- J. Li, Q. Vuong, S. Liu, M. Liu, K. Ciosek, H. Christensen, and H. Su. Multi-task batch reinforcement learning with metric learning. Advances in Neural Information Processing Systems, 33:6197–6210, 2020.
- L. Li, Y. Huang, M. Chen, S. Luo, D. Luo, and J. Huang. Provably improved context-based offline meta-rl with attention and contrastive learning. *arXiv* preprint arXiv:2102.10774, 2021a.
- L. Li, R. Yang, and D. Luo. Focal: Efficient fully-offline meta-reinforcement learning via distance metric learning and behavior regularization. In *International Conference on Learning Representations*, 2021b.
- X. L. Li and P. Liang. Prefix-tuning: Optimizing continuous prompts for generation. In Proceedings of the 59th Annual Meeting of the Association for Computational Linguistics and the 11th International Joint Conference on Natural Language Processing (Volume 1: Long Papers), pages 4582–4597, 2021.
- N. Mishra, M. Rohaninejad, X. Chen, and P. Abbeel. Meta-learning with temporal convolutions. *arXiv preprint arXiv:1707.03141*, 2(7):23, 2017.
- E. Mitchell, R. Rafailov, X. B. Peng, S. Levine, and C. Finn. Offline meta-reinforcement learning with advantage weighting. In *International Conference on Machine Learning*, pages 7780–7791. PMLR, 2021.
- A. v. d. Oord, Y. Li, and O. Vinyals. Representation learning with contrastive predictive coding. arXiv preprint arXiv:1807.03748, 2018.
- V. H. Pong, A. V. Nair, L. M. Smith, C. Huang, and S. Levine. Offline meta-reinforcement learning with online self-supervision. In *International Conference on Machine Learning*, pages 17811– 17829. PMLR, 2022.
- C. Raffel, N. Shazeer, A. Roberts, K. Lee, S. Narang, M. Matena, Y. Zhou, W. Li, and P. J. Liu. Exploring the limits of transfer learning with a unified text-to-text transformer. *The Journal of Machine Learning Research*, 21(1):5485–5551, 2020.
- K. Rakelly, A. Zhou, C. Finn, S. Levine, and D. Quillen. Efficient off-policy meta-reinforcement learning via probabilistic context variables. In *International conference on machine learning*, pages 5331–5340. PMLR, 2019.
- S. Reed, K. Zolna, E. Parisotto, S. G. Colmenarejo, A. Novikov, G. Barth-maron, M. Giménez, Y. Sulsky, J. Kay, J. T. Springenberg, et al. A generalist agent. *Transactions on Machine Learning Research*, 2022.
- T. Schaul, D. Horgan, K. Gregor, and D. Silver. Universal value function approximators. In *International conference on machine learning*, pages 1312–1320. PMLR, 2015.
- S. Shalev-Shwartz, S. Shammah, and A. Shashua. Safe, multi-agent, reinforcement learning for autonomous driving. *arXiv preprint arXiv:1610.03295*, 2016.
- N. Tishby and N. Zaslavsky. Deep learning and the information bottleneck principle. In 2015 ieee information theory workshop (itw), pages 1–5. IEEE, 2015.
- N. Tishby, F. Pereira, W. Bialek, B. Hajek, and R. Sreenivas. Proceedings of the 37th annual allerton conference on communication, control and computing. In *Proceedings ao the 37-th Annual Allerton Conference on Communication, Control and Computing, chapter The information bottleneck method*, pages 368–377, 1999.
- N. Tishby, F. C. Pereira, and W. Bialek. The information bottleneck method. *arXiv preprint physics/0004057*, 2000.
- E. Todorov, T. Erez, and Y. Tassa. Mujoco: A physics engine for model-based control. In 2012 IEEE/RSJ international conference on intelligent robots and systems, pages 5026–5033. IEEE, 2012
- L. Van der Maaten and G. Hinton. Visualizing data using t-sne. *Journal of machine learning research*, 9(11), 2008.

- J. X. Wang, Z. Kurth-Nelson, D. Tirumala, H. Soyer, J. Z. Leibo, R. Munos, C. Blundell, D. Kumaran, and M. Botvinick. Learning to reinforcement learn. *arXiv preprint arXiv:1611.05763*, 2016.
- Y. Wu, G. Tucker, and O. Nachum. Behavior regularized offline reinforcement learning. *arXiv* preprint arXiv:1911.11361, 2019.
- M. Xu, Y. Shen, S. Zhang, Y. Lu, D. Zhao, J. Tenenbaum, and C. Gan. Prompting decision transformer for few-shot policy generalization. In *international conference on machine learning*, pages 24631–24645. PMLR, 2022.
- R. W. Yeung. Information theory and network coding. Springer Science & Business Media, 2008.
- T. Yu, D. Quillen, Z. He, R. Julian, K. Hausman, C. Finn, and S. Levine. Meta-world: A benchmark and evaluation for multi-task and meta reinforcement learning. In *Conference on robot learning*, pages 1094–1100. PMLR, 2020a.
- T. Yu, G. Thomas, L. Yu, S. Ermon, J. Y. Zou, S. Levine, C. Finn, and T. Ma. Mopo: Model-based offline policy optimization. *Advances in Neural Information Processing Systems*, 33:14129–14142, 2020b.
- H. Yuan and Z. Lu. Robust task representations for offline meta-reinforcement learning via contrastive learning. In *International Conference on Machine Learning*, pages 25747–25759. PMLR, 2022.
- H. Zhang, H. Yu, J. Zhao, D. Zhang, C. Huang, H. Zhou, X. Zhang, and C. Ye. How to fine-tune the model: Unified model shift and model bias policy optimization. In *Thirty-seventh Conference on Neural Information Processing Systems*, 2023.
- M. Zhao, P. Abbeel, and S. James. On the effectiveness of fine-tuning versus meta-reinforcement learning. *Advances in Neural Information Processing Systems*, 35:26519–26531, 2022a.
- T. Z. Zhao, J. Luo, O. Sushkov, R. Pevceviciute, N. Heess, J. Scholz, S. Schaal, and S. Levine. Offline meta-reinforcement learning for industrial insertion. In 2022 International Conference on Robotics and Automation (ICRA), pages 6386–6393. IEEE, 2022b.
- R. Zhou, C.-X. Gao, Z. Zhang, and Y. Yu. Generalizable task representation learning for offline meta-reinforcement learning with data limitations. *arXiv preprint arXiv:2312.15909*, 2023.
- L. Zintgraf, K. Shiarli, V. Kurin, K. Hofmann, and S. Whiteson. Fast context adaptation via metalearning. In *International Conference on Machine Learning*, pages 7693–7702. PMLR, 2019.

Pseudo-Code

Algorithm 1 UNICORN Meta-training

Input: Offline Datasets $X = \{X^i\}_{i=1}^{N_{train}}$, training tasks $M = \{M^i\}_{i=1}^{N_{train}}$, initialized learned policy π_{ω} , Q function Q_{ψ} , context encoder q_{ϕ} , decoder p_{θ} , hyper-parameter α , β , task batch size N_{tbatch}

- 1: while not done do
- Sample task batch $\{M^j\}_{j=1}^{N_{tbatch}} \sim M$ and the corresponding replay buffer $\mathcal{R}=$ $\{X^j\}_{j=1}^{N_{tbatch}} \sim \boldsymbol{X}$
- for step in each iter do 3:
- // Train the context encoder and decoder Sample context $\{c^j\}_{j=1}^{N_{tbatch}} \sim \mathcal{R}$ 4:
- 5:
- Obtain task embeddings $\{ m{z}^j \sim q_\phi(m{z}|m{c}^j) \}_{j=1}^{N_{tbatch}}$ Compute $\mathcal{L}_{ ext{UNICORN}} = \mathcal{L}_{ ext{recon}} + \frac{\alpha \beta 1}{(1 \alpha) \beta} \mathcal{L}_{ ext{FOCAL}}$ 6:
- 7:
- Update ϕ , θ to minimize $\mathcal{L}_{\text{UNICORN}}$ 8:
- // Train the actor and critic 9:
- Detach the task embeddings $\{z^j\}_{j=1}^{N_{tbatch}}$ 10:
- Sample training data $\{d^j\}_{j=1}^{N_{tbatch}} \sim \mathcal{R}$ 11:
- 12: Compute $\mathcal{L}_{actor}, \mathcal{L}_{critic}$
- Update ω, ψ to minimize $\mathcal{L}_{actor}, \mathcal{L}_{critic}$ 13:
- 14: end for
- 15: end while

Algorithm 2 UNICORN Meta-testing

Input: Offline Datasets $X = \{X^i\}_{i=1}^{N_{test}}$, testing tasks $M = \{M^i\}_{i=1}^{N_{test}}$, learned policy π_{ω} , context encoder q_{ϕ}

- 1: **for** each M^i **do**
- Sample context $c^i \sim X^i$
- Obtain task embedding $z^i \sim q_{\phi}(z|c^i)$
- Rollout policy $\pi_{\omega}(\boldsymbol{a}|\boldsymbol{s},\boldsymbol{z}^i)$ for evaluation 4:
- 5: end for

B **Proofs**

Theorem B.1. Let \equiv denote equality up to a constant

$$\underbrace{I(oldsymbol{Z};oldsymbol{X}_t|oldsymbol{X}_b)}_{primary\ causality} \quad \leq \quad I(oldsymbol{Z};oldsymbol{M}) \quad \leq \quad \underbrace{I(oldsymbol{Z};oldsymbol{X})}_{primary\ +\ lesser\ causality}$$

holds up to a constant, where

- 1. $\mathcal{L}_{FOCAL} \equiv -I(\boldsymbol{Z}; \boldsymbol{X}).$
- 2. $\mathcal{L}_{CORRO} \equiv -I(\boldsymbol{Z}; \boldsymbol{X}_t | \boldsymbol{X}_b)$.
- 3. $\mathcal{L}_{CSRO} > (\lambda 1)I(\mathbf{Z}; \mathbf{X}) \lambda I(\mathbf{Z}; \mathbf{X}_t | \mathbf{X}_b)$.

Proof. Assuming 2, $I(\mathbf{Z}; \mathbf{X}_t | \mathbf{X}_b) \equiv -\mathcal{L}_{\text{CORRO}} \leq I(\mathbf{Z}; \mathbf{M})$ is shown in the Theorem 4.1. of CORRO [Yuan and Lu, 2022] and GENTLE [Zhou et al., 2023] with strong assumptions. We hereby

15

present a proof with minimal assumptions. Given $I(Z; M; X_b) \ge 0$ in Assumption 3.2, we have

$$\begin{split} I(\boldsymbol{Z};\boldsymbol{M}) &= I(\boldsymbol{Z};\boldsymbol{M}|\boldsymbol{X}_b) + I(\boldsymbol{Z};\boldsymbol{M};\boldsymbol{X}_b) \\ &\geq I(\boldsymbol{Z};\boldsymbol{M}|\boldsymbol{X}_b) \\ &= I(\boldsymbol{M};\boldsymbol{Z},\boldsymbol{X}_t|\boldsymbol{X}_b) - I(\boldsymbol{M};\boldsymbol{X}_t|\boldsymbol{Z},\boldsymbol{X}_b) \\ &= \underbrace{I(\boldsymbol{Z};\boldsymbol{M}|\boldsymbol{X}_t,\boldsymbol{X}_b)}_{0 \text{ by } \boldsymbol{M} \to \boldsymbol{X} \to \boldsymbol{Z}} + I(\boldsymbol{M};\boldsymbol{X}_t|\boldsymbol{X}_b) - I(\boldsymbol{M};\boldsymbol{X}_t|\boldsymbol{Z},\boldsymbol{X}_b) \\ &= I(\boldsymbol{M};\boldsymbol{X}_t|\boldsymbol{X}_b) - I(\boldsymbol{M};\boldsymbol{X}_t|\boldsymbol{Z},\boldsymbol{X}_b) \\ &= I(\boldsymbol{M};\boldsymbol{X}_t|\boldsymbol{X}_b) - H(\boldsymbol{X}_t|\boldsymbol{Z},\boldsymbol{X}_b) + H(\boldsymbol{X}_t|\boldsymbol{M},\boldsymbol{Z},\boldsymbol{X}_b) \\ &\geq I(\boldsymbol{M};\boldsymbol{X}_t|\boldsymbol{X}_b) - H(\boldsymbol{X}_t|\boldsymbol{Z},\boldsymbol{X}_b) \\ &= \underbrace{I(\boldsymbol{M};\boldsymbol{X}_t|\boldsymbol{X}_b) - H(\boldsymbol{X}_t|\boldsymbol{Z},\boldsymbol{X}_b)}_{\text{const}} \\ &\equiv I(\boldsymbol{Z};\boldsymbol{X}_t|\boldsymbol{X}_b) + \underbrace{I(\boldsymbol{X}_t;\boldsymbol{X}_b)}_{\text{const}} \\ &\equiv I(\boldsymbol{Z};\boldsymbol{X}_t|\boldsymbol{X}_b), \end{split}$$

as desired. The third and fourth lines are obtained by direct application of the chain rule of mutual information [Yeung, 2008]. All mutual information terms without Z are held constant in the fully offline scenario.

 $I(Z; M) \le I(Z; X)$ is a direct consequence of the Data Processing Inequality [Yeung, 2008] and the Markov chain $M \to X \to Z$ in Assumption 3.2. We now prove the three claims regarding FOCAL, CORRO and CSRO:

1.
$$\mathcal{L}_{\text{FOCAL}} \equiv -I(\boldsymbol{Z}; \boldsymbol{X}).$$

$$I(\boldsymbol{Z}; \boldsymbol{X}) := \mathbb{E}_{\boldsymbol{x}, \boldsymbol{z}} \left[\log \left(\frac{p(\boldsymbol{z}, \boldsymbol{x})}{p(\boldsymbol{z}) p(\boldsymbol{x})} \right) \right]$$

$$= \mathbb{E}_{\boldsymbol{x}, \boldsymbol{z}} \left[\log \left(\frac{1}{\frac{p(\boldsymbol{z})}{p(\boldsymbol{z}|\boldsymbol{x})} |\mathcal{M}|} \right) \right] + \log(|\mathcal{M}|)$$

$$= \mathbb{E}_{\boldsymbol{x}, \boldsymbol{z}} \left[\log \left(\frac{1}{\frac{p(\boldsymbol{z})}{p(\boldsymbol{z}|\boldsymbol{x})} |\mathcal{M}| \mathbb{E}_{\boldsymbol{x}} \left[\frac{p(\boldsymbol{z}|\boldsymbol{x})}{p(\boldsymbol{z})} \right]} \right) \right] + \log(|\mathcal{M}|)$$

$$\approx \mathbb{E}_{\boldsymbol{x}, \boldsymbol{z}} \left[\log \left(\frac{1}{\frac{p(\boldsymbol{z})}{p(\boldsymbol{z}|\boldsymbol{x})} \sum_{M^i \in \mathcal{M}} \mathbb{E}_{\boldsymbol{x}^i \sim X^i} \left[\frac{p(\boldsymbol{z}|\boldsymbol{x}^i)}{p(\boldsymbol{z})} \right]} \right) \right] + \log(|\mathcal{M}|)$$

$$= \mathbb{E}_{\boldsymbol{x}, \boldsymbol{z}} \left[\log \left(\frac{\frac{p(\boldsymbol{z}|\boldsymbol{x})}{p(\boldsymbol{z})}}{\sum_{M^i \in \mathcal{M}} \mathbb{E}_{\boldsymbol{x}^i \sim X^i} \left[\frac{p(\boldsymbol{z}|\boldsymbol{x}^i)}{p(\boldsymbol{z})} \right]} \right) \right] + \log(|\mathcal{M}|)$$

$$= \mathbb{E}_{\boldsymbol{x}, \boldsymbol{z}} \left[\log \left(\frac{h(\boldsymbol{x}, \boldsymbol{z})}{\sum_{M^i \in \mathcal{M}} h(\boldsymbol{x}^i, \boldsymbol{z})} \right) \right] + \log(|\mathcal{M}|)$$

The first term on RHS is precisely the supervised contrastive learning objective introduced by a variant of FOCAL [Li et al., 2021a], which is equivalent to the negative distance metric learning loss \mathcal{L}_{FOCAL} with the effect of pushing away embeddings of different tasks while pulling together those from the same task. Therefore we have

$$I(\boldsymbol{Z}; \boldsymbol{X}) = \mathbb{E}_{\boldsymbol{x}, \boldsymbol{z}} \left[\log \left(\frac{h(\boldsymbol{x}, \boldsymbol{z})}{\sum_{M^i \in \mathcal{M}} h(\boldsymbol{x}^i, \boldsymbol{z})} \right) \right] + \text{const}$$

 $\equiv -\mathcal{L}_{\text{FOCAL}}.$

2.
$$\mathcal{L}_{CORRO} \equiv -I(\boldsymbol{Z}; \boldsymbol{X}_t | \boldsymbol{X}_b)$$
.

$$\begin{split} I(\boldsymbol{Z}; \boldsymbol{X}_{t} | \boldsymbol{X}_{b}) &:= \mathbb{E}_{\boldsymbol{x}_{t}, \boldsymbol{x}_{b}, \boldsymbol{z}} \left[\log \left(\frac{p(\boldsymbol{z}, \boldsymbol{x}_{t} | \boldsymbol{x}_{b})}{p(\boldsymbol{z} | \boldsymbol{x}_{b}) p(\boldsymbol{x}_{t} | \boldsymbol{x}_{b})} \right) \right] \\ &= \mathbb{E}_{\boldsymbol{x}_{t}, \boldsymbol{x}_{b}, \boldsymbol{z}} \left[\log \left(\frac{1}{\frac{p(\boldsymbol{z} | \boldsymbol{x}_{b})}{p(\boldsymbol{z} | \boldsymbol{x}_{t}, \boldsymbol{x}_{b})} | \mathcal{M}|} \right) \right] + \log(|\mathcal{M}|) \\ &= \mathbb{E}_{\boldsymbol{x}_{t}, \boldsymbol{x}_{b}, \boldsymbol{z}} \left[\log \left(\frac{1}{\frac{p(\boldsymbol{z} | \boldsymbol{x}_{b})}{p(\boldsymbol{z} | \boldsymbol{X})} | \mathcal{M} | \mathbb{E}_{\mathcal{M}^{*} \in \mathcal{M}} \left[\frac{p(\boldsymbol{z} | \boldsymbol{x}_{t}^{*}, \boldsymbol{x}_{b})}{p(\boldsymbol{z} | \boldsymbol{x}_{b})} \right]} \right) \right] + \log(|\mathcal{M}|) \\ &\approx \mathbb{E}_{\boldsymbol{x}_{t}, \boldsymbol{x}_{b}, \boldsymbol{z}} \left[\log \left(\frac{1}{\frac{p(\boldsymbol{z} | \boldsymbol{x}_{t}, \boldsymbol{x}_{b})}{p(\boldsymbol{z} | \boldsymbol{x}_{t}, \boldsymbol{x}_{b})}} \sum_{\mathcal{M}^{*} \in \mathcal{M}} \frac{p(\boldsymbol{z} | \boldsymbol{x}_{t}^{*}, \boldsymbol{x}_{b})}{p(\boldsymbol{z} | \boldsymbol{x}_{b})} \right) \right] + \log(|\mathcal{M}|) \\ &= \mathbb{E}_{\boldsymbol{x}_{t}, \boldsymbol{x}_{b}, \boldsymbol{z}} \left[\log \left(\frac{\frac{p(\boldsymbol{z} | \boldsymbol{x}_{t}, \boldsymbol{x}_{b})}{p(\boldsymbol{z} | \boldsymbol{x}_{b})}} \right) \right] + \log(|\mathcal{M}|) \\ &= \mathbb{E}_{\boldsymbol{x}_{t}, \boldsymbol{x}_{b}, \boldsymbol{z}} \left[\log \left(\frac{\frac{p(\boldsymbol{z} | \boldsymbol{x}_{t}, \boldsymbol{x}_{b})}{p(\boldsymbol{z})}}{\sum_{\mathcal{M}^{*} \in \mathcal{M}} \frac{p(\boldsymbol{z} | \boldsymbol{x}_{t}^{*}, \boldsymbol{x}_{b})}{p(\boldsymbol{z})}} \right) \right] + \log(|\mathcal{M}|) \\ &= \mathbb{E}_{\boldsymbol{x}, \boldsymbol{z}} \left[\log \left(\frac{h(\boldsymbol{x}, \boldsymbol{z})}{\sum_{\mathcal{M}^{*} \in \mathcal{M}} h(\boldsymbol{x}^{*}, \boldsymbol{z})} \right) \right] + \log(|\mathcal{M}|) \\ &= -\mathcal{L}_{\text{CORRO}}. \end{split}$$

3. $\mathcal{L}_{CSRO} \geq (\lambda - 1)I(\mathbf{Z}; \mathbf{X}) - \lambda I(\mathbf{Z}; \mathbf{X}_t | \mathbf{X}_b)$.

The CLUB loss in Eqn 6 operates as a upper bound of $I(\mathbf{Z}; \mathbf{X}_b)$ [Cheng et al., 2020]. By Eqn 5 we have

$$\mathcal{L}_{\text{CSRO}} = \mathcal{L}_{\text{FOCAL}} + \lambda L_{\text{CLUB}}$$

$$\geq \mathcal{L}_{\text{FOCAL}} + \lambda I(\boldsymbol{Z}; \boldsymbol{X}_b)$$

$$= \mathcal{L}_{\text{FOCAL}} + \lambda \underbrace{(I(\boldsymbol{Z}; \boldsymbol{X}) - I(\boldsymbol{Z}; \boldsymbol{X}_t | \boldsymbol{X}_b))}_{\text{chain rule of mutual information}}$$

$$\stackrel{1}{=} -I(\boldsymbol{Z}; \boldsymbol{X}) + \lambda (I(\boldsymbol{Z}; \boldsymbol{X}) - I(\boldsymbol{Z}; \boldsymbol{X}_t | \boldsymbol{X}_b))$$

$$= (\lambda - 1)I(\boldsymbol{Z}; \boldsymbol{X}) - \lambda I(\boldsymbol{Z}; \boldsymbol{X}_t | \boldsymbol{X}_b).$$

C Further Experiments

C.1 Hyper-parameter Study of $\frac{\alpha\beta-1}{(1-\alpha)\beta}$

We experiment with $\frac{\alpha\beta-1}{(1-\alpha)\beta}$ from 0 to 10, as shown in Figure 6. We observe that UNICORN has an optimal $\frac{\alpha\beta-1}{(1-\alpha)\beta}$ in all environments. This observation suggests that it is insufficient to use either FOCAL loss or reconstruction loss alone, emphasizing the necessity of their combination proposed in Eqn 7 and 8.

Intuitively, for tasks differ in transition dynamics, the lesser causality $I(\boldsymbol{Z};\boldsymbol{X}_b)$ should be higher since the state distribution $\mu_{\pi}(\boldsymbol{s})$ vary across tasks even with the same behavior policy π . This indicates that the optimal proportion of FOCAL loss in Eqn 12 should be greater on these environments, as it maximizes $I(\boldsymbol{Z};\boldsymbol{X})$ along with the primary causality $I(\boldsymbol{Z};\boldsymbol{X}_t|\boldsymbol{X}_b)$. Such thought experiment is verified in this study. We record the optimal $\frac{\alpha\beta-1}{(1-\alpha)\beta}$ of all benchmarks in Table 5, demonstrating that for tasks differ in *reward function* (Ant-Dir, HalfCheetah-Dir) and *transition dynamics* (Hopper-Param, Walker-Param), the optimal value of $\frac{\alpha\beta-1}{(1-\alpha)\beta}$ is around 0.1 and 1 respectively. The fact that the

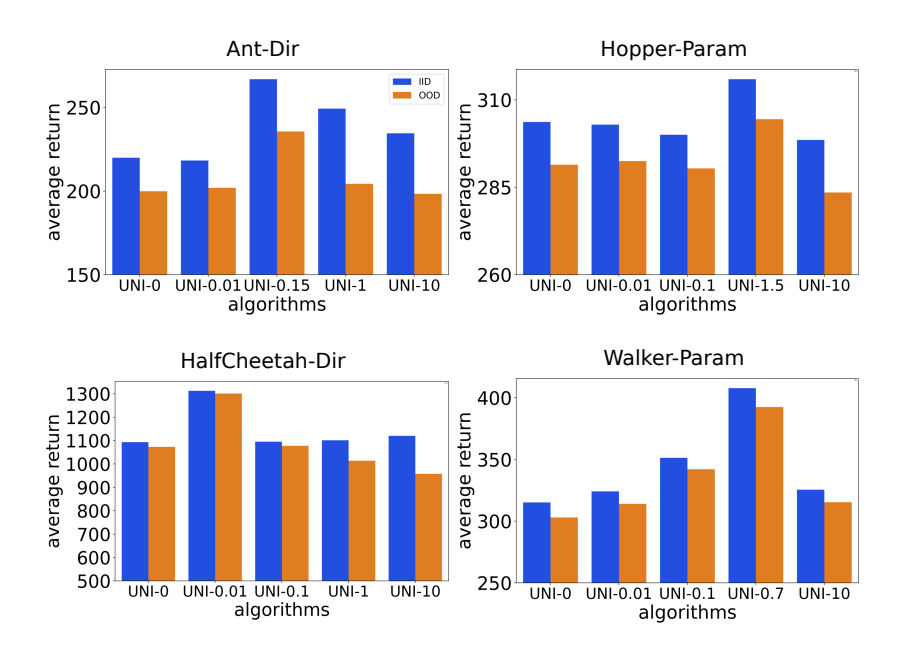


Figure 6: Hyper-parameter study results in all environments, each result is averaged over 6 random seeds.

optimal $\frac{\alpha\beta-1}{(1-\alpha)\beta}$ does not vanish for Ant-Dir and HalfCheetah-Dir suggests that the lesser causality $I(\boldsymbol{Z};\boldsymbol{X}_b)$ should be nonzero even when all tasks share the same transition dynamics. We conjecture this is partially due to the fact that the behavior policy we use for each task is also trained on that task, which leads to task-dependent state distribution $\mu_{\pi}(s)$. However, this applies to the IID setting only.

C.2 UNICORN-0: A Label-free Version

When $\frac{\alpha\beta-1}{(1-\alpha)\beta}$ equals zero, UNICORN task representation learning reduces to the minimization of the reconstruction loss only, which becomes a *label-free* algorithm (i.e., it does not require the knowledge of task identities/labels to optimize, as opposed to the contrastive learning in previous methods). We name this special case UNICORN-0, which is equivalent to a concurrent method GENTLE [Zhou et al., 2023]. For a fair comparison, we use a variant of a Bayesian OMRL method BOReL [Dorfman et al., 2021] that does not utilize oracle reward functions, as a label-free baseline. At test time, we modify BOReL to use offline datasets rather than the online data collected by interacting with the environment to infer the task information³. As shown in Table 4, UNICORN-0 is also competitive with BOReL.

Table 4: UNICORN-0 compared to another label-free COMRL method, BOReL, on Ant-Dir.

Algorithm	Ant-Dir				
Augoriumi	IID	OOD			
UNICORN-0	219.88±16.24	199.86±9.26			
BOReL	206.4±17.93	186.55±9.54			

³Experiment shows that the usage of offline dataset rather than online data has little effect on the results of BOReL.

C.3 Visualization of Task Representations

For better interpretation, we visualize the task representations by 2D projection of the embedding vectors via t-SNE [Van der Maaten and Hinton, 2008]. For each test task, we generate a trajectory using each policy in $\{\pi_{\beta}^{i,t}\}_{i,t}$ and infer their task representations z. This setting aligns with our OOD experiments in the main text.

Since the UNICORN objective operates as a convex combination of the reconstruction loss (UNICORN-0) and the FOCAL loss, we compare representations of UNICORN to these two extremes. As shown in Figure 7, compared to UNICORN-0, UNICORN provides evidently more distinguishable task representations for OOD data, emphasizing the necessity of joint optimization with the FOCAL loss. On the other hand, despite the seemingly higher quality of task representations of FOCAL, the performance of FOCAL is much worse than UNICORN. We speculate that since FOCAL blindly separates embeddings from different tasks, it may fail to capture shared structure between similar tasks, whereas UNICORN is able to do so by generative modeling via the reconstruction loss.



Figure 7: The 2D projection of the learned task representation space in Ant-Dir. Points are uniformly sampled from out-of-distribution data. Tasks of given goals from 0 to 6 are mapped to rainbow colors, ranging from purple to red.

C.4 More on UNICORN-DT

We provide the learning curves of the results in Section 5.1 here. As shown in Figure 8, UNICORN-DT demonstrates both the higher convergence speed and the higher asymptotic performance compared to the vanilla Prompt-DT.

D Experimental Details

Table 5 lists the necessary hyper-parameters that we used to produce the experimental results.

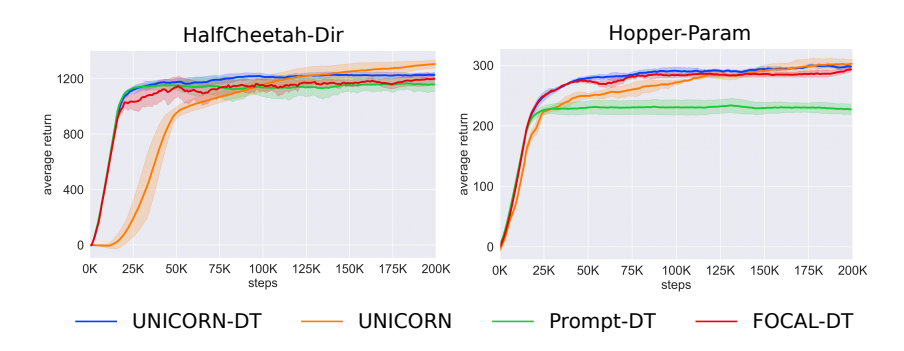


Figure 8: Test returns of UNICORN-DT against UNICORN and Prompt-DT on 2 benchmarks. The learning curve is averaged by 6 random seeds.

Table 5: Configurations and hyper-parameters used in the training process.

Configurations	Ant-Dir	HalfCheetah-Dir	HalfCheetah-Vel	Hopper-Param	Walker-Param	Reach		
dataset size	1e5	2e5	2e5	3e5	4.5e5	1e5		
task representation dimension	5	5	5	40	32	2		
optimal $\frac{\alpha\beta-1}{(1-\alpha)\beta}$	0.15	0.01	0.15	1.5	0.7	0.3		
training steps			200k					
task batch size	16							
RL batch size			256					
context training size			200			500		
learning rate			3e-4					
RL network width			256					
RL network depth			3					
encoder width		64		12	28	64		